The Journal of Immunology

RESEARCH ARTICLE | JUNE 15 2014

Il-1β and Reactive Oxygen Species Differentially Regulate Neutrophil Directional Migration and Basal Random Motility in a Zebrafish Injury–Induced Inflammation Model

Bo Yan; ... et. al

J Immunol (2014) 192 (12): 5998–6008.
https://doi.org/10.4049/jimmunol.1301645

Il-1β and Reactive Oxygen Species Differentially Regulate Neutrophil Directional Migration and Basal Random Motility in a Zebrafish Injury–Induced Inflammation Model

Bo Yan,* Peidong Han,† Lifeng Pan,* Wei Lu,* Jingwei Xiong,† Mingjie Zhang,* Wenqing Zhang,‡ Li Li,§ and Zilong Wen*

During inflammation, the proper inflammatory infiltration of neutrophils is crucial for the host to fight against infections and remove damaged cells and detrimental substances. IL-1β and NADPH oxidase–mediated reactive oxygen species (ROS) have been implicated to play important roles in this process. However, the cellular and molecular basis underlying the actions of IL-1β and ROS and their relationship during inflammatory response remains undefined. In this study, we use the zebrafish model to investigate these issues. We find that, similar to that of NADPH oxidase–mediated ROS signaling, the Il-1β–Myd88 pathway is required for the recruitment of neutrophils, but not macrophages, to the injury-induced inflammatory site, whereas it is dispensable for bacterial-induced inflammation. Interestingly, the Il-1β–Myd88 pathway is independent of NADPH oxidase–mediated ROS signaling and critical for the directional migration, but not the basal random movement, of neutrophils. In contrast, the NADPH oxidase–mediated ROS signaling is required for both basal random movement and directional migration of neutrophils. We further document that ectopic expression of Il-1β in zebrafish induces an inflammatory disorder, which can be suppressed by anti-inflammatory treatment. Our findings reveal that the Il-1β–Myd88 axis and NADPH oxidase–mediated ROS signaling are two independent pathways that differentially regulate neutrophil migration during sterile inflammation. In addition, Il-1β overexpressing *Tg(hsp70:^{m}il-1β_eGFP;lyz:DsRed2)hkz10t;nz50* transgenic zebrafish provides a useful animal model for the study of chronic inflammatory disorder and for anti-inflammatory drug discovery. *The Journal of Immunology*, **2014, 192: 5998–6008.**

The proper and rapid locomotion of innate immune cells to target sites is extremely important for the success of immune responses (1). Compared to infectious inflammation, in which the signaling network underlying leukocyte behavior and function has been well defined, the study of sterile inflammation remains largely undeveloped. Neutrophils, one of the essential components of innate immune cells, are considered to be a double-edged sword during sterile inflammation. They are the first phagocytes recruited to the sterile inflammation site, and they facilitate the removal of dead/damaged cells and detrimental substances (2, 3). In contrast, dysregulated neutrophilic infiltration is also involved in inflammatory diseases and cancer development (4, 5). Considering the paradoxical roles of neutrophils, it is widely accepted that a well-regulated neutrophil infiltration during inflammatory response is vital for the hosts. However, the cellular and molecular basis that regulates neutrophil recruitment during sterile inflammation is not fully understood. The zebrafish has recently been widely used as an animal model to study immunity, owing to its conserved immune system and imaging and genetic amenability (2, 6–8). Furthermore, because zebrafish process only the innate immune system in the early stage of development (9, 10), they provide an ideal in vivo model to study the functions and behaviors of innate immune cells.

The primary trigger of sterile inflammation is cell death, during which endogenous molecules including damage-associated molecular patterns, proinflammatory cytokines, and chemokines are released to initiate an acute response (11). IL-1β is one of the proinflammatory cytokines involved in infection, reperfusion injury, and various inflammatory diseases (12). In mammals, IL-1β exists as pro–IL-1β in living cells and can be quickly converted into its biologically active form (mature IL-1β) upon caspase-1 cleavage (12), which allows the rapid and robust activation of IL-1β and its downstream signaling cascades. IL-1β functions through binding to its receptor IL-1R, which in turn activates the NF-κB pathway via the adaptor protein MyD88 (13). The activation of the NF-κB pathway induces the expression of inflammatory genes, resulting in inflammation. Despite the understanding of its molecular

*State Key Laboratory of Molecular Neuroscience, Center of Systems Biology and Human Health, Division of Life Science, Hong Kong University of Science and Technology, Kowloon, Hong Kong, China; †Institute of Molecular Medicine, Peking University, Beijing 100871, China; ‡Key Laboratory of Zebrafish Modeling and Drug Screening for Human Diseases of Guangdong Higher Education Institutes, Department of Cell Biology, Southern Medical University, Guangzhou 510515, China; and §Key Laboratory of Freshwater Fish Reproduction and Development, Ministry of Education, State Key Laboratory Breeding Base of Eco-Environments and Bio-Resources of the Three Gorges Area, School of Life Science, Southwest University, Chongqing 400715, China

Received for publication June 21, 2013. Accepted for publication April 11, 2014.

This work was supported by General Research Fund grants from the Research Grants Council of the Hong Kong Special Administrative Region (663111, 663212, HKUST6/CRF/09, HKUST5/CRF/12R, HKUST6/CRF/10, and T13-607/12R), the National Basic Research Program of China (Grant 2012CB945102), and the National Natural Science Foundation of China (Grants 31171403 and 30828020).

Address correspondence and reprint requests to Prof. Zilong Wen or Prof. Li Li, State Key Laboratory of Molecular Neuroscience, Center of Systems Biology and Human Health, Division of Life Science, Hong Kong University of Science and Technology, Clear Water Bay, Kowloon, Hong Kong, China (Z.W.) or Key Laboratory of Freshwater Fish Reproduction and Development, Ministry of Education, State Key Laboratory Breeding Base of Eco-Environments and Bio-Resources of the Three Gorges Area, School of Life Science, Southwest University, Chongqing 400715, China (L.L.). E-mail addresses: zilong@ust.hk (Z.W.) or swu_lili@126.com (L.L.)

The online version of this article contains supplemental material.

Abbreviations used in this article: dpf, d postfertilization; DPI, diphenyleneiodonium; eGFP, enhanced GFP; F, forward; hpa, h postamputation; hpf, h postfertilization; hphs, h post–heat shock; hsp, heat shock protein; ^{m}*il-1β*, mature *il-1β* form; minpa, min postamputation; MO, morpholino; mpo, myeloperoxidase; PIP_3-PIP_2, phosphatidylinositol (3,4,5)-trisphosphate–phosphatidylinositol (4,5)-bisphosphate; PTU, *N*-phenylthiourea; R, reverse; ROS, reactive oxygen species; WISH, whole-mount in situ hybridization.

action, the biological importance of IL-1β in sterile inflammation remains controversial. For example, as expected, *IL-1β*–null mice fail to initiate an acute-phase response in turpentine injection–induced tissue damage (14). Likewise, the immune response to monosodium urate challenging is defective in caspase-1–deficient mice, in which IL-1β maturation is severely impaired (15). These studies suggest that IL-1β is essential for the generation of immune response in response to sterile inflammatory stimuli. This view, however, was challenged by a later study showing that leukocyte response was not compromised in the IL-1β Ab–treated and caspase-1–deficient mice upon stimulation with necrotic cells (16). Thus, further study is needed to clarify the in vivo function of IL-1β during sterile inflammation and define precisely how IL-1β regulates leukocyte infiltration in an in vivo setting.

With its unique advantages of imaging and genetic amenability (2, 6–8), the zebrafish model provides a unique opportunity to tackle this issue. Similar to the mammalian homolog, zebrafish Il-1β was shown to be cleaved by caspase-A and caspase-B, the two homologs of mammalian caspase-1 (17). However, zebrafish Il-1β lacks the typical caspase-1 cleavage site shared by higher vertebrates including humans and mice (18), and instead, it can be cleaved at multiple sites (17). Despite this difference, zebrafish Il-1β preserves its function as a potent proinflammatory cytokine involved in acute inflammatory responses and tissue regeneration (19). Thus, understanding the role of Il-1β in zebrafish during inflammatory response may shed light on its function in mammals.

Besides IL-1β, reactive oxygen species (ROS) has also been suggested in the neutrophil-mediated immune response. Upon the initiation of chemoattraction to the inflammatory site or during phagocytosis, neutrophils produce abundant ROS via a process referred as to "respiration burst" (4). Although the ROS produced during phagocytosis is well known to be involved in the elimination of invading microorganisms, the role of ROS during leukocyte chemotaxis remains elusive. Previous in vitro assays have revealed that H_2O_2, one major component of ROS, can induce murine peritoneal macrophage activation and peritoneal neutrophil chemotactic activity via a Ca^{2+}-mediated manner (20, 21). More recently, using the zebrafish model, it has been demonstrated that H_2O_2 produced by Duox (a member of the NADPH oxidase family) is required for leukocyte recruitment to the injury site (22–24). Yet, the detailed mechanism underlying ROS-mediated leukocyte recruitment and the relationship between ROS and IL-1β signaling during the inflammatory response warrant for further investigation.

In this study, we identified the Il-1β–Myd88 axis as a key pathway in regulating neutrophil recruitment in response to sterile injury, but not to bacterial infection in zebrafish. We demonstrated that the Il-1β–Myd88 axis and ROS pathway function independently to regulate neutrophil migration during injury-induced inflammation. We also showed that the Il-1β–Myd88 pathway regulates directional migration of neutrophils during injury-induced inflammation, but has no effect on the basal random movement. In contrast, the ROS signaling is required for both basal random motility and injury-induced directional migration of neutrophils. We further provided evidence indicating that the action of the Il-1β–Myd88 and ROS pathways involves regulating the polarity of PI3K activity. Finally, we documented that ectopic expression of mature Il-1β in zebrafish leads to an inflammatory disorder that is sensitive to anti-inflammatory treatment.

Materials and Methods

Zebrafish strains and maintenance

The zebrafish strains, including AB, Tg(lyz:DsRed2)nz50, Tg(coro1a:eGFP;lyz:DsRed2)hkz04t;nz50, Tg(hsp70:eGFP;lyz:DsRed2)hkz09t;nz50, Tg(hsp70:^{m}il-1β_eGFP;lyz:DsRed2)hkz10t;nz50, and Tg(β-actin:Hyper)pku326, were raised under standard conditions (2, 25, 26). Embryos were maintained in egg water containing 0.2 mM *N*-phenylthiourea (PTU) (Sigma-Aldrich) to prevent pigment formation (25). The egg water and buffers were freshly filtered through a 0.22-μm Millipore Steritop filter (Millipore), and containers were autoclaved before use.

Chemical and pharmacological treatment

Larvae were incubated in egg water containing 100 μm diphenyleneiodonium (DPI) and 1% DMSO 1 h before tail fin amputation or bacterial injection (23, 24). Diclofenac (1 μm) and dexamethasone (800 μm) treatments of embryos were performed for 12 h before the heat-shock experiment (23, 24, 27).

Morpholino injection

The following morpholinos (MOs; Gene Tools) were injected into one-cell embryos at the indicated final amounts: *il-1β* e6i6 (0.8 pmol), *il-1β* e3i3 (1.6 pmol), *il-1β* Mis_e3i3 MO (1.6 pmol), *myd88* ATG/ e2i2^{hig} (2 pmol/3 pmol), *myd88* ATG/ e2i2^{low} (1 pmol/1.5 pmol), *duox-MO1* (1.6 pmol), *duox-MO2/p53* (1.6 pmol/0.8 pmol), *nox5* i10e11 (0.8 pmol), *cyba* (3.2 pmol), *cyba/nox5* (3.2 pmol/0.8 pmol), and standard control MO (1 pmol). In this work, if there was no specific description, we used *il-1β* MO, *myd88* MO, and *duox* MO to represent *il-1β* e3i3 MO, *myd88* ATG/ e2i2 MO, and *duox-MO1*, respectively. The sequences of the MOs are as follows: *il-1β* e6i6 MO (5′-TAATCATGGAGCACAAACCTTGAGT-3′); *il-1β* e3i3 MO (5′-AAACGTAAAATAACTCACCATTGCA-3′); *il-1β* Mis_e3i3 MO (5′-AAACcTAAtATAAgTCAgCATTGgA-3′); *myd88* atg MO (5′- GGTCTATACTTAACTTTGATGCCAT-3′) (28); *myd88* e2i2 MO (5′-GTTAAACACTGACCCTGTGGATCAT-3′) (29); *duox-MO1* (5′-TAGATTACTACTCACCAACAGCTTA-3′) (30); *duox-MO2* (5′-AGTGAATTAGAGAAATGCACCTTTT-3′) (23); *p53* MO (5′-GCGCCATTGCTTTGCAAGAATTG-3′) (23); *nox5* i10e11 MO (5′-AATGCGTCACCTTTAAAACACACGT-3′); *cyba* MO (5′-ATCATAGCATGTAAGGATACATCCC-3′) (23); and standard control MO (5′-CCTCTTACCTCAGTTACAATTTATA-3′).

Bacterial injection

Escherichia coli cells were harvested by centrifugation at 5000 × *g* for 5 min and resuspended in sterile PBS. The working concentration of *E. coli* was 1.2×10^9/ml, and ~0.06 nl bacterial suspension was injected into 2.5-d postfertilization (dpf) embryos mounted in 1.2% low-melting agarose on glass slides with 0.02% tricaine. Injection was performed on the stage of an Olympus SZX7 ZOOM stereomicroscope (Olympus) with a gas manipulator (Havard Apparatus, Holliston, MA). For bacterial-induced inflammation, *E. coli* cells were s.c. injected into the muscle of fifth somite.

Protein purification and injection

Recombinant protein 6xHis-tagged Cxcl8-l1 was purified accordingly (31). The recombinant 6xHis-tagged Cxcl8-l1 protein (50 pg/embryo) and the same volume of flow-through solution was s.c. injected into the muscle of fifth somite.

Laser injury

The laser injury was performed on Leica SP5 confocal microscope (Leica Microsystems) by scanning a small target region (10–15 μm) at 200 Hz frequency with a 405-nm laser at maximal power for 3–5 min.

DNA expression constructs and transgenic line generation

The modified vector PT2AL200R150G was used for all DNA expression constructs (32). pTol2-*hsp70:*^{m}*il-1β*, pTol2-*hsp70:eGFP*, pTol2-*hsp70:*^{m}*il-1β_eGFP*, and pTol2-*β-actin:Hyper* were generated and injected into one-cell embryos together with transposase mRNA (25 ng/μl). The F1 *Tg(hsp70:eGFP;lyz:DsRed2)hkz09t;nz50*, *Tg(hsp70:*^{m}*il-1β_eGFP;lyz:DsRed2)hkz10t;nz50*, and *Tg(β-actin:Hyper)pku326* fish were obtained by mating the founders with *Tg(lyz:DsRed2)nz50*.

RNA extraction and semiquantitative/quantitative RT-PCR

RNA was prepared by using the RNeasy Micro kit (Qiagen), and cDNA was generated with the Superscript III First Strand Synthesis System (Invitrogen). Semiquantitative PCR was performed as described previously (33), whereas quantitative RT-PCR was performed with SYBR Green Supermix (Bio-Rad) (34). The primers used are as follows: il-1β 637-forward (F), 5′-GTACTCAAGGAGATCAGCGG-3′; il-1β-831-reverse (R), 5′-CTCGGTGTCTTTCCTGTCCA-3′; il-1βexon1F, 5′-GATGGCATGCGGGCAATATG-3′; exon4R, 5′-GATGATGACGTTCACCAACTG-3′; myd88e1F, 5′-TCTTGACGGACTGGGAAACTCG-3′; MyD88e5R, 5′-GATTTG-

TAGACGACAGGGATTAGCC-3′; cxcl8-l1-F, 5′-TGTTTTCCTGGC-ATTTCTGACC-3′; cxcl8-l1-R, 5′-TTTACAGTGTGGGCTTGGAGGG-3′; cxcl8-l2-F, 5′-CCACACACACTCCACACACA-3′; cxcl8-l2-R, 5′-CCACT-GAATTGTCCTTTCATCA-3′;ef1a-F: 5′-CTTCTCAGGCTGACTGTGC'3′; and ef1a-R, 5′-CCGCTAGCATTACCCTCC-3′.

In situ hybridization

Whole-mount in situ hybridization (WISH) was performed as described (35). Digoxigenin-labeled full-length antisense RNA probes of *il-1β* (BC098597), *il-6* (JN698962), and *cxcl8-l1* (XM_001342570) were used for WISH.

Tail amputation assay

Embryos were collected in egg water and transferred to new Petri dishes containing sterile filtered egg water with 0.2 mM PTU at 24 h post-fertilization (hpf). A relatively sterile condition was achieved by frequent changes of egg water and petri dish and the rapid removal of the abnormal/dying embryos. The embryos were placed into fresh sterile filtered egg water with 0.02% tricaine (Sigma-Aldrich), and tail fin amputation was performed with a sterile 24-gauge needle. Finally, the amputated embryos were placed in fresh sterile filtered egg water containing 0.2 mM PTU for further analysis.

Live imaging and data analysis

To observe in vivo behaviors of macrophages and neutrophils, the *Tg (coro1a:eGFP;lyz:DsRed2)hkz04t;nz50* line was used (2). The 2–2.5 dpf larvae were mounted in 1.2% low-melting agarose with 0.02% tricaine and 0.2 mM PTU. To monitor H_2O_2 concentration, hyper-ratio imaging was performed using a Leica SP5 confocal microscope (Leica Microsystems). The detection wavelength range was set as 505–565 nm, with excitation at 488 and 405 nm (23). Images were processed by ImageJ software (National Institutes of Health) according to the following procedure: substrate background → transfer to 32-bit format → smoothing → threshold → select Ratio Plus analysis → select Lookup Table using "Blue_Green_Red" → adjust display range via "Brightness/Contrast" to produce best signal-to-noise ratio image of interested cells → add calibration bar (36). PHAKT-enhanced GFP (eGFP)/DsRed2 ratio imaging was performed using a 63× water lens and analyzed similarly as described in hyper-ratio imaging.

Video-enhanced differential interference contrast imaging

Video-enhanced differential interference contrast microscopy was performed as described (37).

Heat shock

Tg(hsp70:eGFP;lyz:DsRed2)hkz09t;nz50 and *Tg(hsp70:*^{m}*il-1β_eGFP;lyz:DsRed2)hkz10t;nz50* embryos were raised at 26°C for 3 d to reduce basal activation of the heat-shock promoter (32, 38). Heat-shock treatment was conducted at 39°C for 2 × 2 h with 1-h intervals.

Sequence alignment and prediction of the three-dimensional structure

Sequence alignment was performed using ClustalW2 software (39). A model of the protein's three-dimensional structure was generated using the online Phyre2 server and further optimized by energy minimization using the YASARA server (40, 41).

Statistics

Data are shown as the mean ± SEM. Differences were analyzed by using the two-tailed Student *t* test and considered significant at $p < 0.05$.

Results

Tissue injury activates il-1β signaling

When inflammation occurs, immune cells swiftly migrate to the affected site in response to signaling mediated by cytokines, chemokines, and ROS (2, 3, 11, 23, 24). After inducing inflammation in zebrafish by tail amputation in a relatively sterile condition, we investigated genes that were upregulated as part of the acute response, because these genes were considered to be likely involved in sterile inflammation. As a result, *il-1β* was identified as a candidate. Although *il-1β* mRNA was not detectable by WISH in 2.5-dpf embryos under normal conditions, we found a strong *il-1β* mRNA expression at the wound sites by 2 h postamputation (hpa), and its expression decreased from 4 hpa onwards (Fig. 1A–E). Protein sequence alignment revealed that zebrafish Il-1β has a high degree of similarity to IL-1β of other vertebrate species in both primary sequences and secondary structure (Supplemental Fig. 1A). Based on the mammalian IL-1β, a putative mature zebrafish Il-1β was predicted to have a similar tertiary structure to that of human IL-1β (Supplemental Fig. 1B–D). The predicted putative mature Il-1β protein was shown to have biological activity because the overexpression of the putative mature *il-1β* form (^{m}*il-1β*) resulted in ectopic expression of *il-6* and *cxcl-8-l1* mRNA (Fig. 1F–I), two inflammatory cytokines known to be induced by IL-1β in mammals (42, 43). Our findings indicate that Il-1β is evolutionally conserved and likely to be involved in injury-induced inflammatory responses in zebrafish, which is consistent with the results reported in a recent study (44).

The Il-1β–Myd88 signaling axis is required for the recruitment of neutrophils to the injured site

Inflammation can be divided into two subtypes: sterile inflammation and inflammation associated with infection. To study the role of Il-1β in both types of inflammation, two independent splice-blocking MOs, *il-1β* e3i3 and *il-1β* e6i6, were designed to specifically knock down *il-1β* mRNA (Supplemental Fig. 2A–C, 2I) in *Tg(coro1a:eGFP,lyz:DsRed2)hkz04t,nz50* transgenic zebrafish, in which macrophages and neutrophils can be labeled by different fluorescent colors (2). Because both MOs have identical phenotypes, only results from the *il-1β* e3i3 MO were presented in this study. The embryos injected with *il-1β* MOs (morphants) did not display obvious defects in neutrophil morphology, number, and distribution (Supplemental Fig. 2D, 2E and data not shown). Tail amputation and bacterial injection were then performed in control and *il-1β* morphants. At 2 hpa of the tail fin, ∼10 neutrophils were found in the wound region of 2.5-dpf normal zebrafish. However, a significantly smaller number of neutrophils was observed in *il-1β* morphants (Fig. 2A–C, 2J, Supplemental Fig. 2F). In contrast, the number of neutrophils accumulated at the bacterial injection site was similar in both control and *il-1β* morphants (Fig. 2D–I, 2K, 2L). As a control, sterile PBS was also injected to induce local sterile inflammation. Similar to that of tail amputation, the number of neutrophils accumulating at the site of sterile PBS injection was significantly reduced in the *il-1β* morphants (Fig. 2D–F, 2K). In contrast, Il-1β knockdown had no effect on macrophage recruitment in response to both sterile (injury-induced in this case) inflammation and inflammation associated with infection (Fig. 2A–L, Supplemental Fig. 2F). These data suggest that Il-1β plays a specific role in regulating the recruitment of neutrophils, but not macrophages, during injury-induced inflammation, whereas it is dispensable for infection-elicited neutrophil response.

In mammals, it is known that IL-1β, upon binding to its cognate receptors, activates downstream targets via MyD88 (13). We speculated that a similar mechanism might be used in zebrafish. To test this hypothesis, two MOs, *myd88atg* and *myd88e2i2*, which interfere with *myd88* mRNA translation and splicing, respectively (28, 29), were coinjected to effectively knock down *myd88* expression in zebrafish embryos followed by tail fin amputation and bacterial injection (Supplemental Fig. 2G). As expected, the knockdown of Myd88 expression blocked injury-induced but not bacterial-induced recruitment of neutrophils (Fig. 2M, 2O) without the obvious induction of *il-1β* production (Supplemental Fig. 2H). In contrast, macrophage recruitment was unaffected (Fig. 2N). Consistent with the notion that IL-1β and MyD88 act in the same pathway, neither a low dosage of the *il-1β* nor of *myd88* MO alone could block neutrophil recruitment, but the combination of both was sufficient to do so (Fig. 2M). Fur-

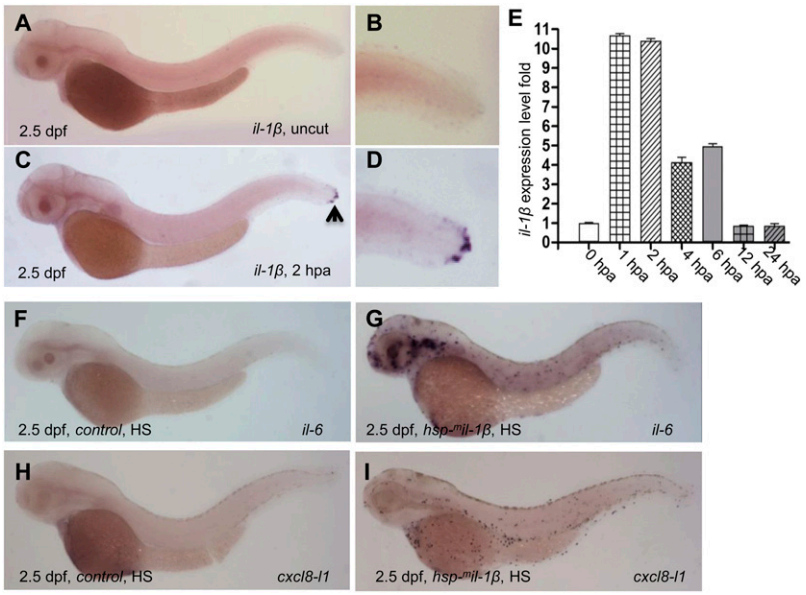

FIGURE 1. Tissue injury initiates *il-1β* signaling. (**A**–**D**) The *il-1β* WISH data of 2.5-dpf embryos before tail amputation and 2 hpa. (**E**) Histogram shows that the *il-1β* RNA level in the tail fin region dramatically increased within the first 2 hpa and decreased thereafter in 52-hpf wild-type embryos. (**F** and **G**) WISH of *il-6* in 2.5-dpf control and heat shock (HS)–induced *il-1β*–overexpression embryos. (**H** and **I**) WISH of *cxcl8-l1* in 2.5-dpf control and HS-induced *il-1β*–overexpression embryos.

thermore, we showed that the expressions of *cxcl8-l1* and *cxcl8-l2*, two chemokines that were recently found to mediate the injury-induced migration of neutrophils in zebrafish (31, 45), were downregulated in both *il-1β* and *myd88* morphants (Fig. 2P, 2Q), and s.c. injection of the recombinant Cxcl8-l1 into the *il-1β* morphants could rescue the migratory defect of neutrophils (Fig. 2R). This result indicates that Cxcl8-l1 acts downstream of Il-1β in the regulation of injury-induced migration of neutrophils. Collectively, these data suggest that the *il-1β–myd88* signaling axis may regulate injury-induced neutrophil directional migration, at least in part, via regulating *cxcl8-l1* expression.

Il-1β–Myd88 and NADPH oxidase–mediated ROS pathways independently regulate neutrophil injury-induced inflammatory response

Recent studies have shown that ROS produced at the wound site by Duox (a member of the NADPH oxidase family) serves as an important cue for the acute leukocytes' (both neutrophils and macrophages) recruitment during injury-induced inflammation (22–24). This prompted us to investigate the relationship between NADPH oxidase–mediated ROS and the Il-1β signaling pathway. To clarify this issue, we first treated fish embryos with DPI, a potent inhibitor of NADPH oxidase–mediated ROS production (22–24), and asked whether it would affect *il-1β* expression upon tail amputation. Results showed that pretreatment of embryos with DPI did not lead to a significant reduction of *il-1β* expression (Fig. 3A, 3B, 3E, 3F, 3I). Instead, it prolonged injury to *il-1β* mRNA expression, as indicated by the positive staining of *il-1β* mRNA in the DPI-treated embryos but not in the untreated controls after 6 hpa (Fig. 3C, 3D, 3G–I), indicating that NADPH oxidase–mediated ROS does not act upstream of *il-1β–myd88* axis. Conversely, we examined the production of H_2O_2, a major ROS product generated at the wound site during sterile inflammation (23, 24), upon the disruption of the *il-1β–myd88* signal axis. To monitor the changes in H_2O_2 concentration in vivo, *Tg (β-actin:Hyper)pku326*, transgenic zebrafish in which a specific H_2O_2 biosensor is ubiquitously expressed (23, 46), were used. As shown in Fig. 3, a rapid increase of H_2O_2 was seen at the wound edges in the control embryos as well as *il-1β* and *myd88* morphants at ~20 min postamputation (minpa) (Fig. 3J). Quantification analysis revealed that the mean hyper-ratios at the wound edges of control embryos, *il-1β* morphants, and *myd88* morphants were ~1.542, 1.581, and 1.594, respectively (Fig. 3K), indicating that the inactivation of the *il-1β–myd88* signaling axis has no significant effect on NADPH oxidase–mediated ROS production. Together, these findings suggest that *il-1β–myd88* and NADPH oxidase–mediated ROS are two independent pathways required for neutrophil recruitment during injury-induced inflammation.

Il-1β–Myd88 and NADPH oxidase–mediated ROS are differentially required for basal random movement and injury-induced directional migration of neutrophils

To further characterize the differences between the Il-1β– and ROS-mediated neutrophil responses, time-lapse analysis was performed to assess different aspects of neutrophil behavior. We found that, at steady state, the neutrophils residing in the tissues were constantly moving within a certain area, presumably patrolling the surrounding tissues to check for damaged cells and infectious agents (Fig. 4B, Supplemental Video 1). This type of movement, which in this study is referred as to basal random movement of neutrophils, appears to be random and is independent of extracellular inflammatory stimuli. Upon tissue injury, neutrophils migrate swiftly to the site of injury via relatively straight migration routes, with an increase of migration directionality index, migration velocity, migration territory, and forward migration distance (Fig. 4A, 4C, 4K, Supplemental Fig. 3A, 3B, Supplemental Video 2). This type of neutrophil movement is directional and depends on extracellular inflammatory stimuli and is therefore referred as to directional migration. We next assessed the migratory behavior of neutrophils in *il-1β* and *myd88* morphants before and after tail amputation. We found that both *il-1β* and *myd88* morphants displayed a basal migratory pattern similar to that of the control morphants under injury-free conditions (Fig. 4D, 4F, Supplemental Fig. 3A, 3B, Supplemental Video 1). However, upon tail amputation, neutrophils rapidly migrated toward the injury site in the control morphants, whereas neutrophils in the *il-1β* and *myd88* morphants moved randomly and failed to reach the injury site, resulting in the reduction of neutrophil number in the wound region (Fig. 4A, 4E, 4G, 4K, 4L, Supplemental Fig. 3A, 3B, Supplemental Videos 2, 3). These data indicate that the *il-1β–myd88* signaling is essential for injury-induced directional migration of neutrophils but is dispensable for the basal random movement of neutrophils. A similar assay was performed to investigate the effect of NADPH oxidase–me-

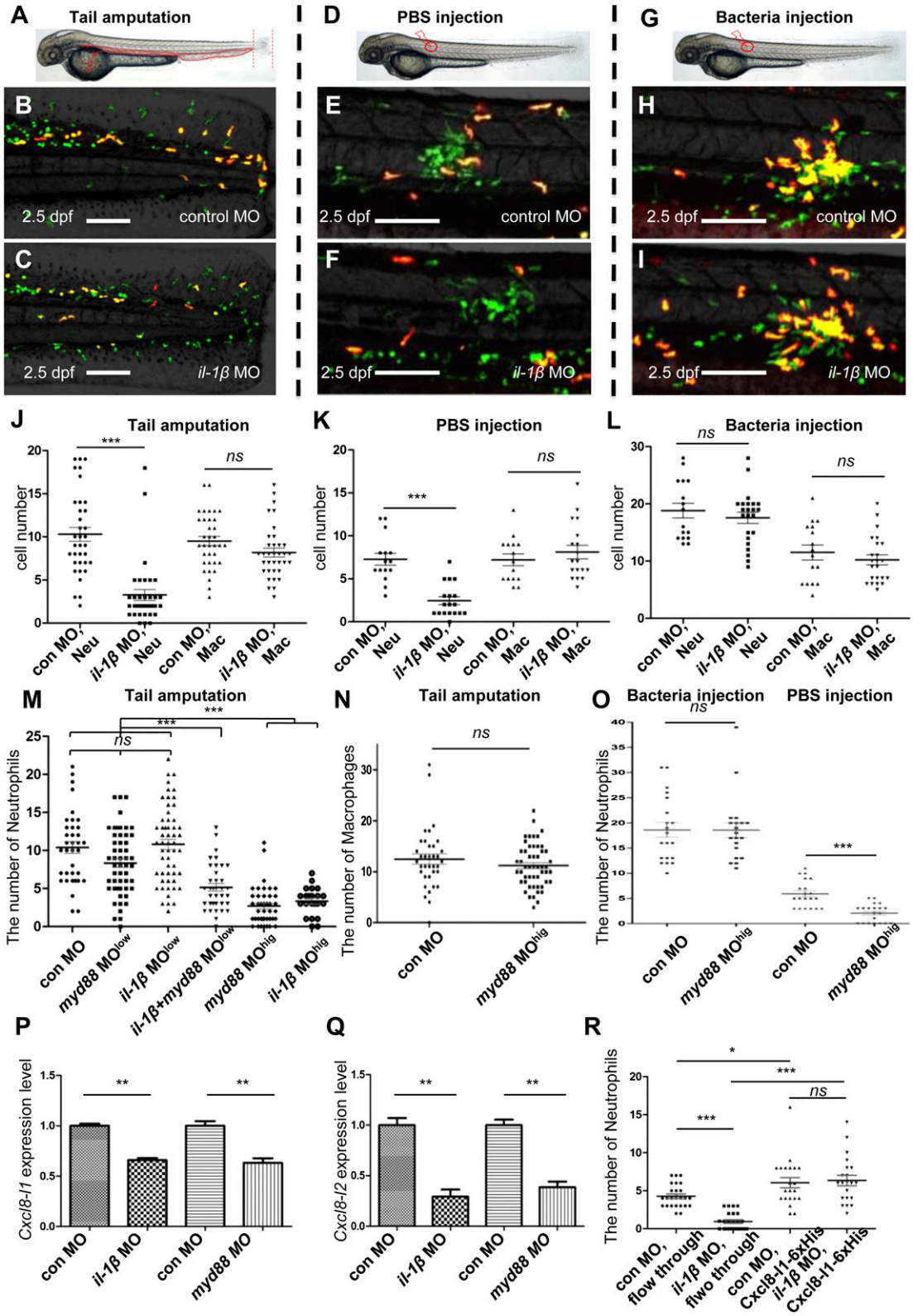

FIGURE 2. The Il-1β–Myd88 axis plays an essential role in injury-induced neutrophil infiltration. (**A**) Schematic view of tail amputation. The wound area is defined as the region between the amputation edge and circulation end. (**D** and **G**) Schematic views of PBS and bacterial injection assay. (**B**, **E**, and **H**) The distribution of neutrophils and macrophages 2 h after the control morphants were subjected to tail amputation, s.c. injection of PBS, and s.c. injection of *E. coli*, respectively. *Tg(coro1a:eGFP;lyz:DsRed2)hkz04t;nz50* transgenic fish were used. Scale bars, 100 μm. (**C**, **F**, and **I**) The distribution of neutrophils and macrophages 2 h after *il-1β* morphants were subjected to tail amputation and PBS and *E. coli* injection into the muscle, respectively. *Tg (coro1a:eGFP;lyz:DsRed2)hkz04t;nz50* was used. Scale bar, 100 μm. (**J** and **K**) Quantification analysis shows that the neutrophil number (Neu) in the wound and the area near the PBS injection site is significantly decreased in the *il-1β* morphants compared with the control (con) morphants, whereas the macrophage (Mac) numbers are comparable in both *il-1β* and control morphants. ***$p < 0.001$. (**L**) Quantification analysis shows that the numbers of both neutrophils and macrophages near the bacterial injection site are comparable in the *il-1β* and control morphants. (**M**) Quantification analysis reveals that the number of neutrophils in the wound at 2 hpa is similar or slightly reduced among the 2.5-dpf embryos injected with low dosage (*Figure legend continues*)

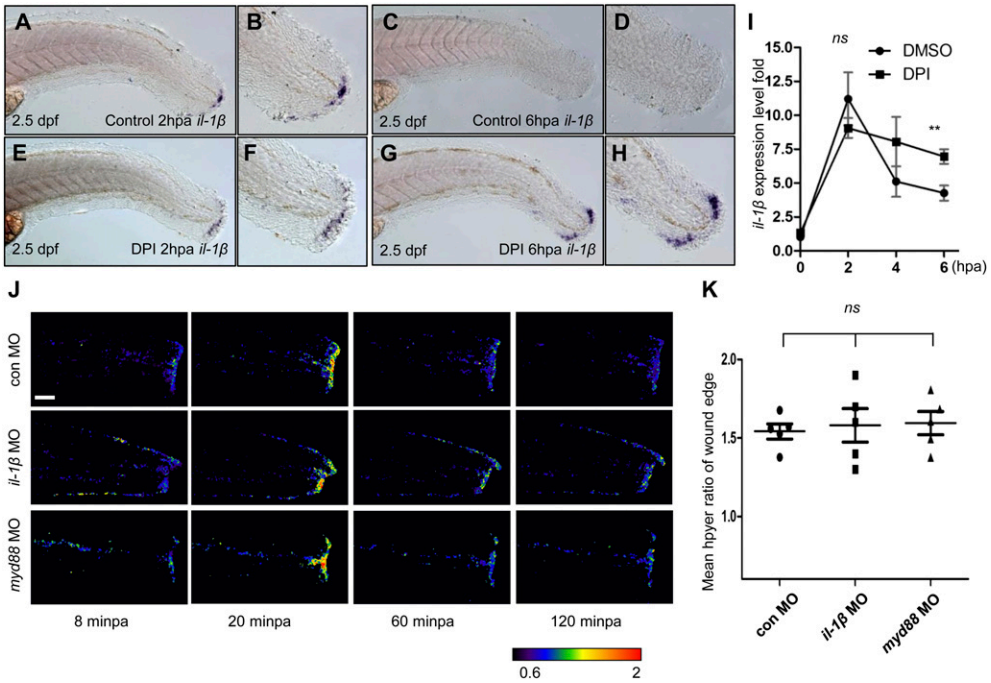

FIGURE 3. Injury-induced *il-1β* mRNA and ROS are produced via two independent pathways. WISH indicates that the *il-1β* mRNA expression is comparable in 2.5-dpf control and DPI-treated embryos at 2 hpa (**A**, **B**, **E**, and **F**), whereas the *il-1β* mRNA expression increases significantly in the DPI-treated embryos at 6 hpa (**C**, **D**, **G**, and **H**). (**I**) Quantitative RT-PCR shows the *il-1β* expression level in the wound of 54-hpf DMSO- and DPI-treated embryos at 0, 2, 4, and 6 hpa. The *il-1β* expression level is normalized with *elf1a* expression. $^{**}p < 0.01$. (**J**) HyPer heat maps indicate the dynamic change of H_2O_2 concentration near the wound edge of 54-hpf control (con), *il-1β*, and *myd88* morphants (MO) at 8, 20, 60, and 120 minpa. Scale bar, 100 μm. (**K**) Quantitative analysis shows that the mean hyper-ratio of wound edge at 20 minpa is similar in 54-hpf control, *il-1β*, and *myd88* MO. A region within 50 μm of the cutting edge was defined for hyper-ratio calculation.

diated ROS signaling on neutrophil behavior. Surprisingly, we found that both basal random migration and injury-induced directional migration of neutrophils were severely impaired in the embryos treated with the NADPH oxidase inhibitor DPI (Fig. 4H, 4I, 4L, Supplemental Video 4). Notably, the directional migration of neutrophils in response to bacterial-induced inflammation was not affected by the DPI treatment (Supplemental Fig. 3C, 3D, Supplemental Video 5). Based on these observations, we speculated that NADPH oxidase–mediated ROS may be also involved in both basal random migration and injury-induced directional migration of neutrophils. To support this argument, we examined the role of all five members—Nox1, Nox2, Nox4, Nox5, and Duox—of NADPH oxidase family (23, 47) by MO knockdown analysis. Because Nox 1, -2, and -4 share one common subunit, Cyba (23, 47), we therefore first knocked down *cyba* expression and asked whether the inactivation of *nox1*, *-2*, and *-4* simultaneously would affect the basal random migration of neutrophils in zebrafish. Results showed that the suppression of *cyba* expression did not affect the basal random migration of neutrophils (Fig. 4M). Likewise, knocking down either *nox5* or *duox* alone did not perturb the basal random migration of neutrophils, although all of the MOs effectively blocked the expression of their targeted genes (Fig. 4M, Supplemental Fig. 2L, and data not shown). However, the inactivation of Nox (Nox1, -2, -4, and -5 together) clearly reduced the basal random movement of neutrophils (Fig. 4J, 4M, Supplemental Video 4). Taken together, these results indicate that NADPH oxidase–mediated ROS is required for both basal random migration and injury-induced directional migration of neutrophils, whereas *il-1β–myd88* is predominantly involved in injury-induced directional migration of neutrophils.

The basal random movement and injury-induced directional migration of neutrophils require the establishment of PI3K activity polarity

It is known that the establishment of PI3K activity polarity is essential for the regulation of neutrophil mobilization (48–50). We therefore tested whether the neutrophil migration defect in the *il-1β* morphants and DPI-treated embryos was caused by the disruption of PI3K activity polarity. We used the myeloperoxidase (*mpo*) promoter-directed PHAKT-eGFP expression system to monitor the PI3K activity (51) by measuring the phosphatidylinositol (3,4,5)-trisphosphate–phosphatidylinositol (4,5)-bisphosphate (PIP_3-PIP_2) level in the subcellular compartment of neutrophils during basal random movement and wound-induced directional

of *il-1β* MO (*il-1β* MO^{low}), *myd88* MO (*myd88* MO^{low}), or the control (con) MO, whereas the number of neutrophils in the wound of 2.5-dpf embryos injected with high dosage of *myd88* MO (*myd88*^{hig} MO) or *il-1β* (*il-1β* MO^{hig}) at 2 hpa is significantly reduced. $^{***}p < 0.001$. (**N**) Quantification analysis indicates that the number of macrophages in the wound at 2 hpa is comparable in the 2.5-dpf embryos injected with high dosage of *myd88* MO (*myd88* MO^{hig}) and the con MO. (**O**) Quantification analysis shows that although the number of neutrophils near the PBS injection site in the *myd88* MO^{hig} decreases significantly, the number of neutrophils in the bacterial injection site is comparable in the 2.5-dpf *myd88* MO^{hig} and con MO. $^{***}p < 0.001$. (**P** and **Q**) Quantitative RT-PCR analysis shows a reduction of *cxcl8-l1* and *cxcl8-l2* expression in the wound region in the 54-hpf *il-1β* and *myd88* morphants at 2 hpa. The expression level of *cxcl8-l1* and *cxcl8-l2* is normalized with *elf1a* RNA. $^{**}p < 0.01$. (**R**) Quantification analysis shows that the injury-induced neutrophil recruitment defect in the 54-hpf *il-1β* morphants can be rescued by the s.c. injection of recombinant Cxcl8-l1-6xHis but not control (con) flow-through solution. $^{*}p < 0.05$, $^{***}p < 0.001$.

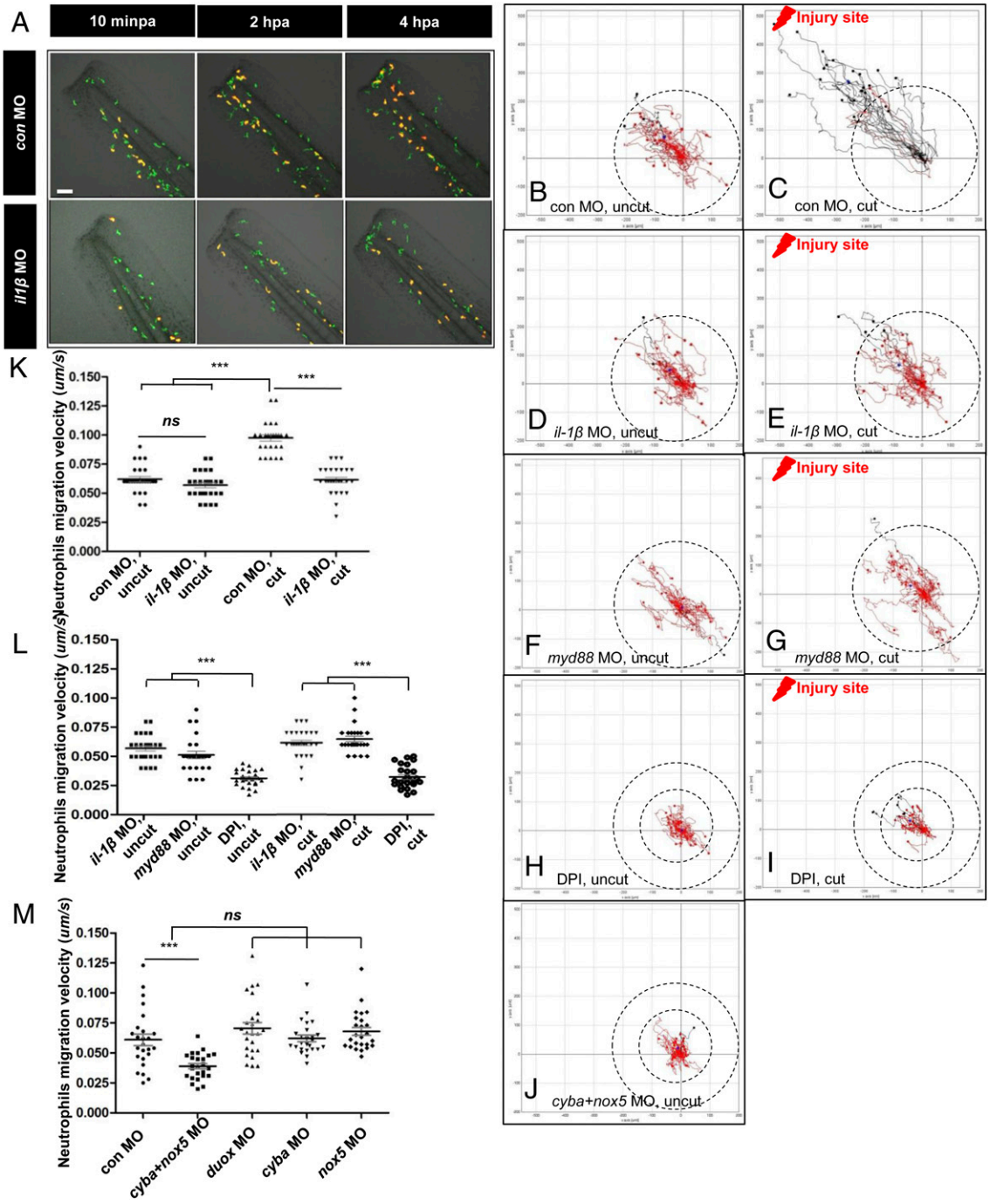

FIGURE 4. Distinctive roles of Il-1β–Myd88 and NADPH oxidase–mediated ROS in the regulation of neutrophil behaviors under normal and injury-induced inflammatory conditions. (**A**) The representative frames (10 minpa, 2 hpa, and 4 hpa) from a 4-h time-lapse video after tail amputation in the 54-hpf *Tg(coro1a:eGFP;lyz:DsRed2)hkz04t;nz50* embryos injected with *il-1β* MO and control (con) MO. Scale bar, 100 μm. (**B**–**J**) The injury-induced migration tracks of the neutrophils from 10 minpa to the time they reach the wound edge (if the neutrophils cannot reach the wound edge, 2.5 hpa is the maximum time for tracing) in 54-hpf neutrophils injected with the *il-1β*, *myd88*, and con MOs. Only actively moving neutrophils (migration speed >0.015 μm/s was considered as moving neutrophil) are followed, and each panel consists of ≥25 neutrophils from 5 embryos. The origin represents the initial position of an individual neutrophil, and the black/red dots represent the final position of each track. Red represents the tracks with the directionality ≤0.4 μm, whereas black represents the tracks with the directionality >0.4 μm. Blue dot represents the center of gravity of the final position of every neutrophil. The black dashed circles are drawn to facilitate the comparison of the area of territory of neutrophil migration. (**K** and **L**) Statistic data of neutrophil migration velocity in embryos injected with the con, *il-1β*, or *myd88* MOs (B–G) and DPI-treated or untreated embryos (H, I) before and after tail amputation. ***$p < 0.001$. (**M**) Statistical data of neutrophil migration velocity in the 54-hpf injury-free embryos injected with the con, *duox*, *cyba*, *nox5*, or *cyba+nox5* MOs. ***$p <$ 0.001.

migration. In control embryos (without injury) in which neutrophils moved randomly, a transient enrichment of PIP_3-PIP_2 was observed in the leading edge (Fig. 5A, Supplemental Video 6); however, PIP_3-PIP_2 enrichment also frequently emerged spontaneously in other regions of the cells, sometimes in the lagging edge, leading to the rapid change of the moving direction of those neutrophils (Fig. 5A, Supplemental Video 6). In the case of tissue injury, the activated neutrophils migrated rapidly toward the

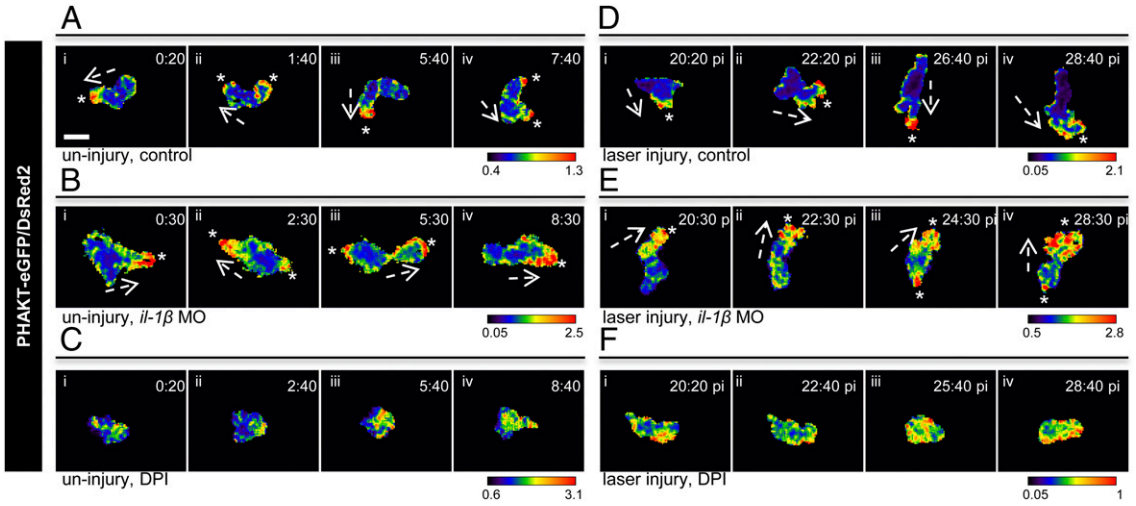

FIGURE 5. PHAKT-eGFP/DsRed2 ratio imaging indicates the distinctive PIP_3-PIP_2 distributions in directional migrating and random moving neutrophils. (**A**–**C**) Time-lapse images of PHAKT-eGFP/DsRed2 ratio reveal the dynamic subcellular localization of PIP_3-PIP_2 in the neutrophils of the 54-hpf injury-free embryos treated with DPI or injected with the *il-1β* and control MOs. In the *il-1β* morphants and control embryos, the PIP_3-PIP_2 signals are detected in multiple regions of a random moving neutrophil, and their subcellular localization changes constantly during their movement (A, B), whereas in the DPI-treated embryos, PIP_3-PIP_2 cannot polarize in the neutrophils (C). The white arrows indicate the neutrophil migration direction, whereas the white asterisks indicate the enrichment points of PIP_3-PIP_2. Scale bar, 10 μm. (**D**–**F**) Time-lapse images of PHAKT-eGFP/DsRed2 ratio indicate the dynamic subcellular localization of PIP_3-PIP_2 in the neutrophils of the 54-hpf injured embryos treated with DPI or injected with the *il-1β* and control MOs. In the control embryos, the PIP_3-PIP_2 signals are localized persistently at the leading edge of the neutrophils (D), whereas in the *il-1β* morphants, the PIP_3-PIP_2 signals are detected in multiple regions of the random moving neutrophils and their subcellular localization changes constantly (E). In the DPI-treated embryos, there is no obvious PIP_3-PIP_2 polarization in the neutrophils (F). The white arrows indicate the neutrophil migration direction, whereas the white asterisks indicate the enrichment points of PIP_3-PIP_2. Scale bar, 10 μm.

wound, accompanied by a long-lasting enrichment of PIP_3-PIP_2 in the leading edge (Fig. 5D, Supplemental Video 6). Spontaneous appearance of PIP_3-PIP_2–enriched signal was not detected in other regions of the cells. Thus, the persisted PI3K activity polarity in the leading edge is essential for the directional migration of neutrophils. In the *il-1β* morphants, however, this long-lasting enrichment of PIP_3-PIP_2 in the leading edge of migrating neutrophils was no longer maintained, and the distribution of PIP_3-PIP_2 polarity in those cells was similar to that of randomly migrating neutrophils observed in the control embryos (Fig. 5B, 5E, Supplemental Video 6). As expected, DPI treatment of embryos blocked the establishment of PI3K activity polarity in neutrophils (Fig. 5C, 5F, Supplemental Video 6). Collectively, these results suggest that NADPH oxidase–mediated ROS and *il-1β–myd88* pathways regulate basal random movement and injury-induced directional migration of neutrophils via modulating the establishment of PI3K activity polarity.

Overexpression of Il-1β induces a systemic inflammation in zebrafish

It is well known that various kinds of human inflammatory diseases are closely associated with the dysregulation of Il-1β (12, 52). We were therefore keen to establish a zebrafish inflammatory disease model by simply overexpressing *il-1β*. To do so, we generated transgenic zebrafish in which a ^{m}Il-1β–eGFP fusion protein was overexpressed via the heat shock protein (*hsp*) 70 promoter (26, 32, 38). The resulting stable transgenic line *Tg(hsp70:^{m}il-1β_eGFP;lyz:DsRed2)hkz10t;nz50* was used to analyze the effect of the Il-1β overexpression on neutrophil behavior. To reduce basal expression of ^{m}Il-1β–eGFP protein, the transgenic embryos were raised at 26°C for 3 d and then subjected to heat-shock treatment at 39°C for a 2 × 2-h incubation. As shown in Fig. 6, the overall number of neutrophils and their distribution pattern were very similar between the control *Tg(hsp70:eGFP;lyz:DsRed2)hkz09t;nz50* and the Il-1β–overexpressing *Tg(hsp70:^{m}il-1β_eGFP;lyz:DsRed2)hkz10t;nz50* embryos before heat-shock treatment (Fig. 6A–D, I). In contrast, after 2-h post–heat shock (hphs) treatment to induce ectopic expression of ^{m}Il-1β_eGFP fusion protein (Fig. 6G), the embryos displayed an abnormal distribution and increased neutrophil number, particular in the upper region of the trunk (boxed region) (Fig. 6E–J). By 12 hphs, the number of circulating neutrophils was also drastically increased in these embryos (Fig. 6I, 6K, Supplemental Video 7). These phenotypes share some common features with human inflammatory disorders, and thus, the *Tg(hsp70:^{m}il-1β_eGFP;lyz:DsRed2)hkz10t;nz50* transgenic line could be used as an animal model for developing new therapeutic strategies for the treatment and prevention of human inflammatory disorders. To provide proof-of concept evidence to support such a notion, we tested whether the treatment of *Tg(hsp70:^{m}il-1β_eGFP;lyz:DsRed2)hkz10t;nz50* embryos with diclofenac and dexamethasone, two anti-inflammatory drugs commonly used for clinical treatment of human inflammatory disorders (27, 53, 54), could reduce the inflammation. Result showed that anti-inflammatory treatment with diclofenac and dexamethasone significantly reduced the number of abnormal distributed neutrophils in heat shock–treated *Tg(hsp70:^{m}il-1β_eGFP;lyz:DsRed2)hkz10t;nz50* embryos (Fig. 6J, 6K). As expected, the inhibitory effect was also achieved by DPI treatment, indicating that the inhibition of NADPH oxidase–mediated ROS signaling is sufficient for controlling Il-1β–related inflammatory disorder (Fig. 6J, 6K). Thus, the ^{m}Il-1β_eGFP protein–overexpressing transgenic zebrafish can serve as an animal model for inflammatory disease study and new drug discovery.

Discussion

In this study, we used the genetic and imaging advantages of zebrafish to study in vivo neutrophil behavior during an inflammatory response. We showed that the *il-1β–myd88* pathway by

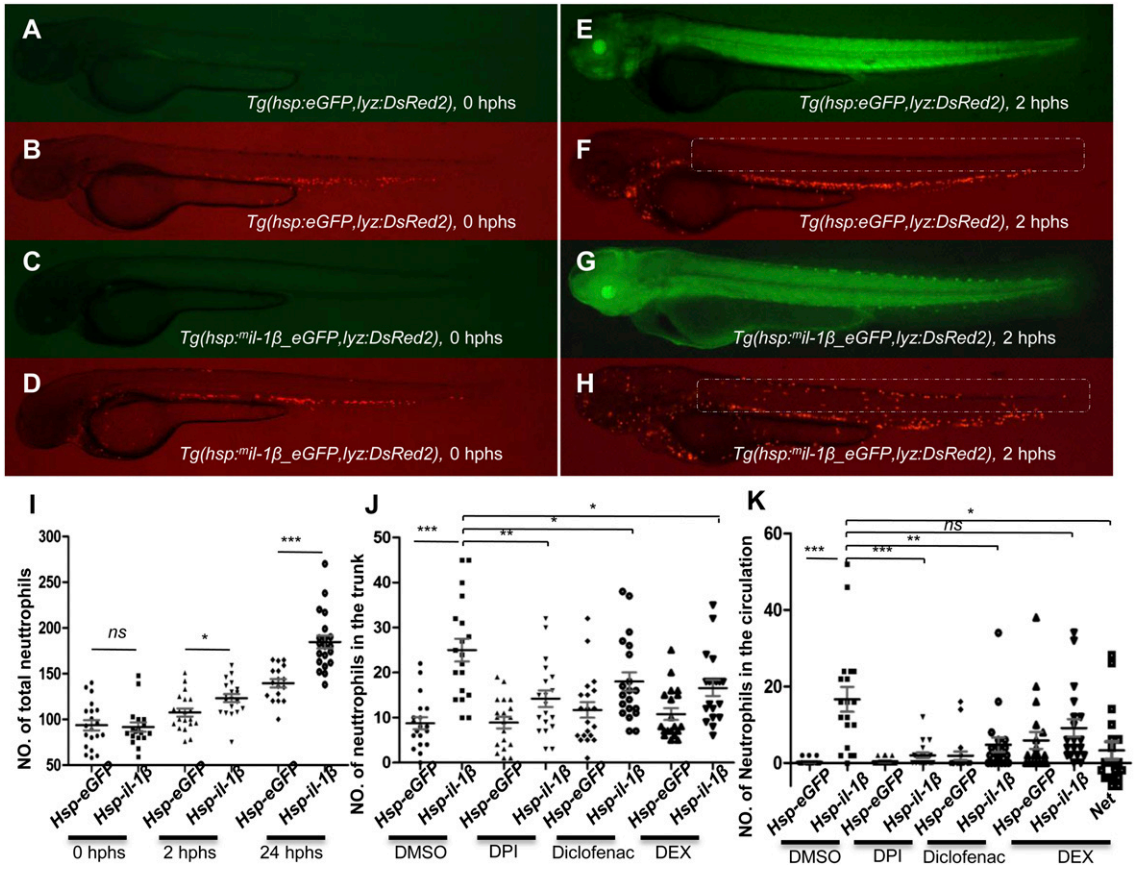

FIGURE 6. Il-1β overexpression leads to systemic inflammation in zebrafish. (**A**–**H**) Immunohistochemistry staining shows that the ectopic overexpression of Il-1β by heat shock leads to an increase of neutrophils in the zebrafish, especially in the head and upper region of the trunk marked by the white dashed line. (A), (B), (E), and (F) are the control *Tg(hsp70:eGFP;lyz:DsRed2)hkz09t;nz50* embryos before and after heat-shock treatment. (C), (D), (G), and (H) are the *Tg(hsp70:*^{m}*il-1β_eGFP;lyz:DsRed2)hkz10t,nz50* embryos before and after heat-shock treatment. (**I**) Quantitative analysis indicates a time-dependent increase of total neutrophil numbers in 3-dpf (26˚C) *Tg(hsp70:*^{m}*il-1β_eGFP;lyz:DsRed2)hkz10t,nz50* embryos 2 and 24 hphs treatment compared with the untreated *Tg(hsp70:*^{m}*il-1β_eGFP;lyz:DsRed2)hkz10t,nz50* embryos (0 hphs) and the control *Tg(hsp70:eGFP;lyz:DsRed2)hkz09t;nz50* embryos. $*p < 0.05$, $***p < 0.001$. (**J**) Quantitative analysis shows an increase of neutrophils in the upper region of the trunk (marked by the dashed line in F and H) of 3-dpf (26˚C) *Tg(hsp70:*^{m}*il-1β_eGFP;lyz:DsRed2)hkz10t,nz50* embryos 2 h after heat-shock (2 hphs) treatment, which can be suppressed by DPI, diclofenac, and dexamethasone (DEX), but not with DMSO treatment. *Tg(hsp70:eGFP;lyz:DsRed2)hkz09t;nz50* embryos are used as the control. $*p < 0.05$, $**p < 0.01$, $***p < 0.001$. (**K**) Quantitative analysis shows an increase of circulating neutrophils in 3-dpf (26˚C) *Tg(hsp70:*^{m}*il-1β_eGFP;lyz:DsRed2)hkz10t,nz50* embryos 12 h after heat-shock (2 hphs) treatment, which can be suppressed by treatment with DPI, diclofenac, and DEX, but not DMSO. Of note, DEX treatment alone slightly increases the circulating neutrophils in the control embryos; thus, Net represents the number of circulating neutrophils in *Tg(hsp70:*^{m}*il-1β_eGFP;lyz:DsRed2)hkz10t,nz50* embryos subtracted from the number of circulating neutrophils in the control *Tg(hsp70:eGFP;lyz:DsRed2)hkz09t;nz50* embryos. $*p < 0.05$, $**p < 0.01$, $***p < 0.001$.

using MO knockdown is required for injury-induced neutrophil but not bacterial infection–induced neutrophil recruitment. We further demonstrated that the *il-1β–myd88* axis and NADPH oxidase–mediated ROS pathway are differentially required for basal random movement and injury-induced directional migration of neutrophils. Although MO knockdown is a transient and incomplete inactivation of the targeted genes and has a nonspecific toxic effect (55), the MOs used in this study are highly specific and have minimal toxic effect, as well documented by others (23, 28–30) and ourselves. We believe that the phenotypes we have observed in our study will likely represent the loss-of-function of the targeted genes. Further studies with specific mutant fish, especially in larvae and adult, will provide new insight into the understanding of the regulation of neutrophils in response to tissue injury.

Our results demonstrate that the *il-1β–myd88* signaling axis is critical for injury-induced directional migration of neutrophils, but it is dispensable for their basal random movement. Although the assays are not done under germ-free conditions, they are carried out under relatively clean conditions by the use of sterilized egg water, solutions, and containers as well as rapid removal of dying embryos. Nonetheless, under these relatively clean conditions, the inflammatory response induced by injury is very similar to that under germ-free conditions: less *il-1β* production, fewer neutrophil infiltrations, and shorter proinflammation process compared with those under conventional conditions (56). We therefore believe our findings are likely to represent those under germ-free conditions. In contrast, NADPH oxidase–mediated ROS is required for both basal random movement and injury-induced directional migration of neutrophils. Our results further suggest that whereas Duox is predominantly involved in injury-induced directional migration of neutrophils, Nox (Nox1, -2, -4, and -5) is required for basal random movement of neutrophils. These findings suggest that basal random movement and injury-induced directional migration of neutrophils are regulated by a distinct signaling pathway. The relationship between basal random movement and directional migration remains unclear at this moment. Given the fact that bacterial-induced neutrophil recruitment is not interfered with by DPI treatment, we speculate that basal random movement is not a prerequisite for inflammation-induced directional migration of neutrophils.

Our findings also reveal that the establishment of transient and persistent PI3K activity polarity in the leading edge of the cells is essential for the basal random movement and injury-induced directional migration of neutrophils. The fact that the suppression of NADPH oxidase–mediated ROS and the *il-1β–myd88* axis has a different effect on the basal random movement and injury-induced directional migration of neutrophils indicates that the establishment of transient and persistent PI3K activity polarity is regulated by distinct signaling pathways involving NADPH oxidase–mediated ROS production and *il-1β–myd88* activation. Although Il-1β and ROS signaling are independent in terms of *il-1β* and ROS production during the injury-induced inflammatory response, they appear to regulate injury-induced neutrophil directional migration via a common downstream event, the establishment of persistent PI3K activity polarity in the leading edge, which requires the activation of both NADPH oxidase–mediated ROS and *il-1β–myd88* pathways. The precise mechanisms underlying the induction of PI3K activity polarity by NADPH oxidase–mediated ROS and *il-1β–myd88* remain largely undefined. One of the downstream signaling molecules could be Ca^{2+}. Previous studies have revealed that there is a temporal and spatial colocalization of PIP_3-PIP_2 and increased Ca^{2+} concentration at the leading edge, and ROS have also been shown to evoke a Ca^{2+} transient (20, 57). We speculate that NADPH oxidase–mediated ROS production may cause an increase of Ca^{2+} concentration, which in turn leads to the activation of PI3K in the leading edge. In addition to Ca^{2+}, inflammatory chemokine *cxcl8-l* (31, 45) is another potential downstream molecule involved in injury-induced neutrophil migration. Because injury-induced *cxcl8-l1 and cxcl8-l2* expression is blocked upon the inactivation of the *il-1β–myd88* axis, and the supplementation of recombinant Cxcl8-l1 protein is sufficient to rescue the neutrophil migratory defect in the *il-1β* knockdown embryos, we therefore believe that the *il-1β–myd88* axis regulates the neutrophil directional migration by controlling Cxcl8 production, which in turn establishes the polarity of PI3K activity through the G-protein–coupled receptors CXCR1 and CXCR2 (58, 59).

Finally, we have generated the *Tg(hsp70:^{m}il-1β_eGFP;lyz:DsRed2)hkz10t,nz50* transgenic fish, which develop a systemic inflammation as indicated by the increase of circulating and tissue neutrophils in an inducible manner. Consistent with the previous results obtained from the transiently *il-1β*–overexpressing embryos, the RNA expression levels of inflammatory cytokines *il-6* and *cxcl8-l1* are also significantly increased in the *il-1β*–overexpressing *Tg(hsp70:^{m}il-1β_eGFP;lyz:DsRed2)hkz10t,nz50* line compared with those in the control *Tg(hsp70:eGFP;lyz:DsRed2)hkz09t,nz50* line (data not shown). This heat shock–induced systemic inflammation can be relieved by the inhibition of the ROS pathway with anti-inflammatory drugs, which is consistent with our findings showing that the activation of both NADPH oxidase–mediated ROS and *il-1β–myd88* pathways is required for neutrophil recruitment during a sterile inflammatory response. These findings imply that the activation of the *il-1β–myd88* axis, at least under the condition of Il-1β overexpression, can turn on, via an unknown mechanism, NADPH oxidase–mediated ROS signaling, resulting in inflammation. Finally, given the fact that current conventional nonsteroidal anti-inflammatory drugs mainly disrupt the cyclooxygenase pathway (60), our findings also suggest that the inhibition of either Il-1β or ROS signaling is sufficient to block sterile inflammation, and perhaps a combinatory inhibition of both pathways can provide a much greater effect. We also believe that *Tg(hsp70:^{m}il-1β_eGFP,lyz:DsRed2)hkz10t,nz50* fish will provide a model system for studying human immune disease and drug discovery.

Acknowledgments

We thank Dr. P. Crosier for sharing the *Tg(lyz:Dsred2)nz50* transgenic line, Dr. A. Huttenlocher for providing the mpo-PHAKT-eGFP/mCherry construct, Drs. M. Sarris and P. Herbomel for providing the pCAG-Cxcl8-l1-6xHis construct and technical suggestions, Drs. Jin Xu and Hao Jin for insightful discussion, and Kaichun Xu, Tienan Wang, Yi Wu, and Nishanth S. Iyengar for help during data preparation and for proofreading the manuscript.

Disclosures

The authors have no financial conflicts of interest.

References

1. Luster, A. D., R. Alon, and U. H. von Andrian. 2005. Immune cell migration in inflammation: present and future therapeutic targets. *Nat. Immunol.* 6: 1182–1190.
2. Li, L., B. Yan, Y. Q. Shi, W. Q. Zhang, and Z. L. Wen. 2012. Live imaging reveals differing roles of macrophages and neutrophils during zebrafish tail fin regeneration. *J. Biol. Chem.* 287: 25353–25360.
3. Ellett, F., L. Pase, J. W. Hayman, A. Andrianopoulos, and G. J. Lieschke. 2011. mpeg1 promoter transgenes direct macrophage-lineage expression in zebrafish. *Blood* 117: e49–e56.
4. Nathan, C. 2006. Neutrophils and immunity: challenges and opportunities. *Nat. Rev. Immunol.* 6: 173–182.
5. Sun, Z., and P. Yang. 2004. Role of imbalance between neutrophil elastase and alpha 1-antitrypsin in cancer development and progression. *Lancet Oncol.* 5: 182–190.
6. Henry, K. M., C. A. Loynes, M. K. Whyte, and S. A. Renshaw. 2013. Zebrafish as a model for the study of neutrophil biology. *J. Leukoc. Biol.* 94: 633–642.
7. Feng, Y., C. Santoriello, M. Mione, A. Hurlstone, and P. Martin. 2010. Live imaging of innate immune cell sensing of transformed cells in zebrafish larvae: parallels between tumor initiation and wound inflammation. *PLoS Biol.* 8: e1000562.
8. Elks, P. M., F. J. van Eeden, G. Dixon, X. Wang, C. C. Reyes-Aldasoro, P. W. Ingham, M. K. Whyte, S. R. Walmsley, and S. A. Renshaw. 2011. Activation of hypoxia-inducible factor-1α (Hif-1α) delays inflammation resolution by reducing neutrophil apoptosis and reverse migration in a zebrafish inflammation model. *Blood* 118: 712–722.
9. Meijer, A. H., and H. P. Spaink. 2011. Host-pathogen interactions made transparent with the zebrafish model. *Curr. Drug Targets* 12: 1000–1017.
10. Bennett, C. M., J. P. Kanki, J. Rhodes, T. X. Liu, B. H. Paw, M. W. Kieran, D. M. Langenau, A. Delahaye-Brown, L. I. Zon, M. D. Fleming, and A. T. Look. 2001. Myelopoiesis in the zebrafish, *Danio rerio*. *Blood* 98: 643–651.
11. Kono, H., and K. L. Rock. 2008. How dying cells alert the immune system to danger. *Nat. Rev. Immunol.* 8: 279–289.
12. Dinarello, C. A. 1996. Biologic basis for interleukin-1 in disease. *Blood* 87: 2095–2147.
13. Burns, K., F. Martinon, C. Esslinger, H. Pahl, P. Schneider, J. L. Bodmer, F. Di Marco, L. French, and J. Tschopp. 1998. MyD88, an adapter protein involved in interleukin-1 signaling. *J. Biol. Chem.* 273: 12203–12209.
14. Fantuzzi, G., and C. A. Dinarello. 1996. The inflammatory response in interleukin-1 beta-deficient mice: comparison with other cytokine-related knockout mice. *J. Leukoc. Biol.* 59: 489–493.
15. Martinon, F., V. Pétrilli, A. Mayor, A. Tardivel, and J. Tschopp. 2006. Gout-associated uric acid crystals activate the NALP3 inflammasome. *Nature* 440: 237–241.
16. Chen, C. J., H. Kono, D. Golenbock, G. Reed, S. Akira, and K. L. Rock. 2007. Identification of a key pathway required for the sterile inflammatory response triggered by dying cells. *Nat. Med.* 13: 851–856.
17. Vojtech, L. N., N. Scharping, J. C. Woodson, and J. D. Hansen. 2012. Roles of inflammatory caspases during processing of zebrafish interleukin-1β in Francisella noatunensis infection. *Infect. Immun.* 80: 2878–2885.
18. Angosto, D., G. López-Castejón, A. López-Muñoz, M. P. Sepulcre, M. Arizcun, J. Meseguer, and V. Mulero. 2012. Evolution of inflammasome functions in vertebrates: Inflammasome and caspase-1 trigger fish macrophage cell death but are dispensable for the processing of IL-1β. *Innate Immun.* 18: 815–824.
19. Kyritsis, N., C. Kizil, S. Zocher, V. Kroehne, J. Kaslin, D. Freudenreich, A. Iltzsche, and M. Brand. 2012. Acute inflammation initiates the regenerative response in the adult zebrafish brain. *Science* 338: 1353–1356.
20. Klyubin, I. V., K. M. Kirpichnikova, and I. A. Gamaley. 1996. Hydrogen peroxide-induced chemotaxis of mouse peritoneal neutrophils. *Eur. J. Cell Biol.* 70: 347–351.
21. Gamaley, I. A., K. M. Kirpichnikova, and I. V. Klyubin. 1994. Activation of murine macrophages by hydrogen peroxide. *Cell. Signal.* 6: 949–957.
22. Deng, Q., E. A. Harvie, and A. Huttenlocher. 2012. Distinct signalling mechanisms mediate neutrophil attraction to bacterial infection and tissue injury. *Cell. Microbiol.* 14: 517–528.
23. Niethammer, P., C. Grabher, A. T. Look, and T. J. Mitchison. 2009. A tissue-scale gradient of hydrogen peroxide mediates rapid wound detection in zebrafish. *Nature* 459: 996–999.
24. Yoo, S. K., T. W. Starnes, Q. Deng, and A. Huttenlocher. 2011. Lyn is a redox sensor that mediates leukocyte wound attraction in vivo. *Nature* 480: 109–112.

25. Westerfield, M. 1995. *The Zebrafish Book: A Guide for the Laboratory Use of Zebrafish (Danio rerio)*, 3rd Ed. University of Oregon Press, Eugene, OR.
26. Hall, C., M. V. Flores, T. Storm, K. Crosier, and P. Crosier. 2007. The zebrafish lysozyme C promoter drives myeloid-specific expression in transgenic fish. *BMC Dev. Biol.* 7: 42.
27. d'Alençon, C. A., O. A. Peña, C. Wittmann, V. E. Gallardo, R. A. Jones, F. Loosli, U. Liebel, C. Grabher, and M. L. Allende. 2010. A high-throughput chemically induced inflammation assay in zebrafish. *BMC Biol.* 8: 151.
28. Valanne, S., H. Myllymäki, J. Kallio, M. R. Schmid, A. Kleino, A. Murumägi, L. Airaksinen, T. Kotipelto, M. Kaustio, J. Ulvila, et al. 2010. Genome-wide RNA interference in Drosophila cells identifies G protein-coupled receptor kinase 2 as a conserved regulator of NF-kappaB signaling. *J. Immunol.* 184: 6188–6198.
29. Bates, J. M., J. Akerlund, E. Mittge, and K. Guillemin. 2007. Intestinal alkaline phosphatase detoxifies lipopolysaccharide and prevents inflammation in zebrafish in response to the gut microbiota. *Cell Host Microbe* 2: 371–382.
30. Flores, M. V., K. C. Crawford, L. M. Pullin, C. J. Hall, K. E. Crosier, and P. S. Crosier. 2010. Dual oxidase in the intestinal epithelium of zebrafish larvae has anti-bacterial properties. *Biochem. Biophys. Res. Commun.* 400: 164–168.
31. Sarris, M., J. B. Masson, D. Maurin, L. M. Van der Aa, P. Boudinot, H. Lortat-Jacob, and P. Herbomel. 2012. Inflammatory chemokines direct and restrict leukocyte migration within live tissues as glycan-bound gradients. *Curr. Biol.* 22: 2375–2382.
32. Halloran, M. C., M. Sato-Maeda, J. T. Warren, F. Su, Z. Lele, P. H. Krone, J. Y. Kuwada, and W. Shoji. 2000. Laser-induced gene expression in specific cells of transgenic zebrafish. *Development* 127: 1953–1960.
33. Li, L., H. Jin, J. Xu, Y. Shi, and Z. Wen. 2011. Irf8 regulates macrophage versus neutrophil fate during zebrafish primitive myelopoiesis. *Blood* 117: 1359–1369.
34. Zhang, Y., H. Jin, L. Li, F. X. Qin, and Z. Wen. 2011. cMyb regulates hematopoietic stem/progenitor cell mobilization during zebrafish hematopoiesis. *Blood* 118: 4093–4101.
35. Jin, H., J. Xu, and Z. Wen. 2007. Migratory path of definitive hematopoietic stem/progenitor cells during zebrafish development. *Blood* 109: 5208–5214.
36. Kardash, E., J. Bandemer, and E. Raz. 2011. Imaging protein activity in live embryos using fluorescence resonance energy transfer biosensors. *Nat. Protoc.* 6: 1835–1846.
37. Jin, H., L. Li, J. Xu, F. Zhen, L. Zhu, P. P. Liu, M. Zhang, W. Zhang, and Z. Wen. 2012. Runx1 regulates embryonic myeloid fate choice in zebrafish through a negative feedback loop inhibiting Pu.1 expression. *Blood* 119: 5239–5249.
38. Lele, Z., S. Engel, and P. H. Krone. 1997. hsp47 and hsp70 gene expression is differentially regulated in a stress- and tissue-specific manner in zebrafish embryos. *Dev. Genet.* 21: 123–133.
39. Larkin, M. A., G. Blackshields, N. P. Brown, R. Chenna, P. A. McGettigan, H. McWilliam, F. Valentin, I. M. Wallace, A. Wilm, R. Lopez, et al. 2007. Clustal W and Clustal X version 2.0. *Bioinformatics* 23: 2947–2948.
40. Krieger, E., K. Joo, J. Lee, J. Lee, S. Raman, J. Thompson, M. Tyka, D. Baker, and K. Karplus. 2009. Improving physical realism, stereochemistry, and side-chain accuracy in homology modeling: Four approaches that performed well in CASP8. *Proteins* 77(Suppl 9): 114–122.
41. Kelley, L. A., and M. J. Sternberg. 2009. Protein structure prediction on the Web: a case study using the Phyre server. *Nat. Protoc.* 4: 363–371.
42. Kuppner, M. C., S. McKillop-Smith, and J. V. Forrester. 1995. TGF-beta and IL-1 beta act in synergy to enhance IL-6 and IL-8 mRNA levels and IL-6 production by human retinal pigment epithelial cells. *Immunology* 84: 265–271.
43. Khan, I., M. G. Blennerhassett, G. V. Kataeva, and S. M. Collins. 1995. Interleukin 1 beta induces the expression of interleukin 6 in rat intestinal smooth muscle cells. *Gastroenterology* 108: 1720–1728.
44. Ogryzko, N. V., E. E. Hoggett, S. Solaymani-Kohal, S. Tazzyman, T. J. Chico, S. A. Renshaw, and H. L. Wilson. 2014. Zebrafish tissue injury causes upregulation of interleukin-1 and caspase dependent amplification of the inflammatory response. *Dis. Model. Mech.* 7: 259–264.
45. de Oliveira, S., C. C. Reyes-Aldasoro, S. Candel, S. A. Renshaw, V. Mulero, and A. Calado. 2013. Cxcl8 (IL-8) mediates neutrophil recruitment and behavior in the zebrafish inflammatory response. *J. Immunol.* 190: 4349–4359.
46. Belousov, V. V., A. F. Fradkov, K. A. Lukyanov, D. B. Staroverov, K. S. Shakhbazov, A. V. Terskikh, and S. Lukyanov. 2006. Genetically encoded fluorescent indicator for intracellular hydrogen peroxide. *Nat. Methods* 3: 281–286.
47. Bedard, K., and K. H. Krause. 2007. The NOX family of ROS-generating NADPH oxidases: physiology and pathophysiology. *Physiol. Rev.* 87: 245–313.
48. Sánchez-Madrid, F., and M. A. del Pozo. 1999. Leukocyte polarization in cell migration and immune interactions. *EMBO J.* 18: 501–511.
49. Wang, F., P. Herzmark, O. D. Weiner, S. Srinivasan, G. Servant, and H. R. Bourne. 2002. Lipid products of PI(3)Ks maintain persistent cell polarity and directed motility in neutrophils. *Nat. Cell Biol.* 4: 513–518.
50. Chung, C. Y., S. Funamoto, and R. A. Firtel. 2001. Signaling pathways controlling cell polarity and chemotaxis. *Trends Biochem. Sci.* 26: 557–566.
51. Yoo, S. K., Q. Deng, P. J. Cavnar, Y. I. Wu, K. M. Hahn, and A. Huttenlocher. 2010. Differential regulation of protrusion and polarity by PI3K during neutrophil motility in live zebrafish. *Dev. Cell* 18: 226–236.
52. El-Omar, E. M., M. Carrington, W. H. Chow, K. E. McColl, J. H. Bream, H. A. Young, J. Herrera, J. Lissowska, C. C. Yuan, N. Rothman, et al. 2000. Interleukin-1 polymorphisms associated with increased risk of gastric cancer. *Nature* 404: 398–402.
53. Skoutakis, V. A., C. A. Carter, T. R. Mickle, V. H. Smith, C. R. Arkin, J. Alissandratos, and D. E. Petty. 1988. Review of diclofenac and evaluation of its place in therapy as a nonsteroidal antiinflammatory agent. *Drug Intell. Clin. Pharm.* 22: 850–859.
54. Coates, T. D., B. Wolach, D. Y. Tzeng, C. Higgins, R. L. Baehner, and L. A. Boxer. 1983. The mechanism of action of the antiinflammatory agents dexamethasone and Auranofin in human polymorphonuclear leukocytes. *Blood* 62: 1070–1077.
55. Eisen, J. S., and J. C. Smith. 2008. Controlling morpholino experiments: don't stop making antisense. *Development* 135: 1735–1743.
56. Galindo-Villegas, J., D. García-Moreno, S. de Oliveira, J. Meseguer, and V. Mulero. 2012. Regulation of immunity and disease resistance by commensal microbes and chromatin modifications during zebrafish development. *Proc. Natl. Acad. Sci. USA* 109: E2605–E2614.
57. Wei, C., X. Wang, M. Chen, K. Ouyang, L. S. Song, and H. Cheng. 2009. Calcium flickers steer cell migration. *Nature* 457: 901–905.
58. Knall, C., G. S. Worthen, and G. L. Johnson. 1997. Interleukin 8-stimulated phosphatidylinositol-3-kinase activity regulates the migration of human neutrophils independent of extracellular signal-regulated kinase and p38 mitogen-activated protein kinases. *Proc. Natl. Acad. Sci. USA* 94: 3052–3057.
59. Waugh, D. J., and C. Wilson. 2008. The interleukin-8 pathway in cancer. *Clin. Cancer Res.* 14: 6735–6741.
60. Vane, J. R., and R. M. Botting. 1998. Anti-inflammatory drugs and their mechanism of action. *Inflamm. Res.* 47(Suppl 2): S78–S87.